

"This document is intended for publication in the open literature. It is made available on the understanding that it may not be further circulated and extracts may not be published prior to publication of the original, without the consent of the Publications Officer, JET Joint Undertaking, Abingdon, Oxon, OX14 3EA, UK".

"Enquiries about Copyright and reproduction should be addressed to the Publications Officer, JET Joint Undertaking, Abingdon, Oxon, OX14 3EA".

A Predictive Study of the JET Mark II Gas Box Divertor

R Simonini, G Corrigan, G Radford, J Spence, A Taroni, G Vlases

JET Joint Undertaking, Abingdon, Oxon, OX14 3EA, United Kingdom

INTRODUCTION

A principal aim of divertor studies at JET is to develop and verify solutions that are relevant for ITER power exhaust and particle control. The Mark II GB divertor was designed specifically to test the ITER Gas Box concept, and is due to begin operation in mid 1997.

The Mark II GB divertor incorporates a flexible design which allows several configurations to be tested. These include horizontal and vertical targets, and an optional septum of as yet unspecified conductance to neutrals. A third possible variant is one which uses a broad, opaque septum to form a double slot divertor.

The EDGE2D/NIMBUS [1] modelling reported in this paper was undertaken to compare the various configurations from an overall performance standpoint.

The perpendicular transport model used is $D_{\perp}=0.5 \text{ m}^2/\text{s}$, $v_{\text{pinch}}=7.5 \text{ m/s}$, $\chi_i = \chi_e = 1 \text{ m}^2/\text{s}$, constant in space, which has been shown to give reasonable simulations of attached L-mode JET plasmas. The Monte Carlo package contains a detailed model of the divertor volume, and includes pumping and by-pass leakage.

EFFECT OF SEPTUM ON A RECYCLABLE IMPURITY

We consider first the case of a deuterium plasma seeded with nitrogen, assumed to be fully recycling. The results are obtained for an equilibrium configuration ($I_p=4.5\text{MA}$), with vertical targets. Fig. 1 shows parts of the computational mesh adopted, with details of the divertor region. In the model, the vessel and the divertor are made of carbon, while the sub-divertor region is made of iron. Sputtering of wall material is inhibited for the runs with nitrogen. We have performed scans of the density at the separatrix mid-plane, n_s , and impurity radiated power, P_{rad} . The required level of P_{rad} is achieved by changing the content of nitrogen through gas puffing. The pumping efficiency of the cryopumps is taken to be 20% for both deuterium and nitrogen. The conductance of the divertor wall to neutrals has been estimated by Monte Carlo calculations [2]. Neutrals entering the by-pass leaks are re-injected at the bottom of the main chamber, while the pumped deuterium is fed back into the SOL from the top of the vessel. Ions diffusing outside the computational mesh toward the vessel are assumed to be transported along field lines and recycled near the divertor shoulders. Boundary conditions at the edge of

the computational domain toward the walls are $\nabla_{\perp}T=0$ and decay length of $\lambda_n=2.5$ cm for temperature and density, respectively.

Table 1 shows relevant parameters for comparing the effects of the presence and shape of the septum for separatrix density $n_s=2\times 10^{19}$ m⁻³, input power $P_i=P_e=5$ MW uniformly into the edge, and impurity radiated power $P_{rad}=6$ MW.

None of the three configurations seems to have a clear advantage over the others. The small differences listed in Table 1 tend to disappear or even change direction at lower density such as $n_s=1\times 10^{19}$ m⁻³ or at lower radiation power. Note that the distribution of the radiated power, as expressed by the fraction $P_{rad,sol}$, does not mirror the impurity density distribution (N_{sol}^z/N_{tot}^z) because of the limited temperature range where radiation is effective.

Table 1. $n_s=2\times 10^{19}$ m⁻³, $P_i=P_e=5$ MW, $P_{rad}=6$ MW, recycling Nitrogen

Symmetry indicators (SOL averages)

Septum	P_{up} (Pa)	$T_{e,up}$ (eV)	P_{out} (Pa)	$T_{e,out}$ (eV)	P_{in} (Pa)	$T_{e,in}$ (eV)
none	292.8	40.5	87.3	5.9	12.5	1.0
opaque	291.2	40.1	85.2	5.7	16.6	1.2
deep V	297.1	40.7	77.2	4.4	39.8	2.1

Particle and power balance

Septum	N_{sol}^z/N_{tot}^z (%)	S_{sol}^z/S_{tot}^z (%)	$P_{rad,sol}$ %	$Z_{eff,max}$ (sol)	N_z/N_i (%)	$\Gamma_{pump}^{0,i}$ ($10^{21}s^{-1}$)	$\Gamma_{pump}^{0,z}$ ($10^{19}s^{-1}$)
none	66.1	12.1	22.3	1.8	0.92	4.0	7.6
opaque	67.2	7.7	17.3	1.7	0.86	4.0	7.6
deep V	74.1	6.1	17.0	1.8	1.19	4.0	15.4

EFFECT OF SEPTUM ON THE INTRINSIC IMPURITY CARBON

In this case, carbon is produced by sputtering. The dominant process is chemical sputtering, for which we have used the model of Ref.[3]. Fig. 2 shows Z_{eff} along the separatrix for the three cases of septum out, septum in, deep V, for $n_s=2\times 10^{19}$ m⁻³ and $P_i=P_e=5$ MW.

The difference in Z_{eff} , due to additional material sputtered from the carbon structure in the private region, influences the approach to detachment, as illustrated in Table 2. While the mid-plane temperature is nearly the same for the three configurations (about 40 eV), the carbon concentration N_z/N_i increases from 3.7% to 8.8% to 19%, and radiation from 6 MW to 8 MW to 9 MW. In the deep V case, the plasma is fully detached. Note that even though the content of C is much higher, the radiated power is not much higher, again a consequence of the narrow

range of temperatures effective for radiation. A fully detached plasma may not be useful since the SOL becomes more and more transparent to neutrals.

Table 2. Approach to detachment induced by carbon, $n_s=2\times 10^{19}\text{m}^{-3}$, $P_i=P_e=5\text{MW}$

Septum	Γ_{target}^i (10^{23} s^{-1})	$P_{\text{c,target}}$ (MW)	$P_{\text{H,rad}}$ (MW)	$P_{\text{H,ex}}$ (MW)	P_{rad} (MW)	N_Z/N_i (%)
none	3.1	2.4	0.3	0.8	6.3	3.7
opaque	1.7	0.8	0.3	0.5	8.0	8.8
deep V	0.9	0.4	0.2	0.4	8.8	19.4

However, these results depend drastically on the model assumed for chemical sputtering, which is subject to large uncertainties. We have assessed the effect of reducing chemical sputtering by a constant factor. In particular, for the sake of comparison with nitrogen, we have reduced the sputtering yield for carbon to 57% of that given in Ref.[3] so as to radiate 6 MW. While most parameters barely differ, there is a difference in the level of impurities necessary to radiate the required power (N_Z/N_i equals 0.86% with N and 3.6% with C), and the density distribution is also different ($N_{\text{sol}}^Z/N_{\text{tot}}^Z$ equals 67% with N and 38% with C). This is due, at least in part, to the broader radiation efficiency of N as a function of temperature.

The carbon sputtered from the main chamber is not the main cause of SOL contamination. When the sputtering is artificially switched off everywhere except in the divertor, in the case of no septum P_{rad} decreases from 6.3 MW to 5.9 MW, the impurity concentration from 3.7% to 3.3% and the maximum of Z_{eff} from 2 to 1.8.

VERTICAL VS. HORIZONTAL TARGETS

Another geometrical configuration being considered is that with horizontal targets (Fig. 3), for which again the septum makes little difference. It is found however that the horizontal configuration tends to enter less easily into the regime of detachment than the vertical one, by requiring a larger amount of seeded impurity to radiate (1.3% vs. 0.86% for $n_s=2\times 10^{19}$ and $P_{\text{rad}}=6\text{MW}$ with opaque septum), since the recycling of D neutrals from the vertical targets toward the separatrix tends to produce a wider region where radiation is effective. As a consequence, the larger amount of seeded nitrogen required in the horizontal target configuration produces $Z_{\text{eff}} = 2.0$ at the outer mid-plane at the separatrix, whereas $Z_{\text{eff}} = 1.7$ in the vertical one.

The vertical configuration has also the obvious advantage of a wider spreading of the heat load over the target plates. This is especially important at high power. Fig. 4 compares the heat loading along the outer target for $n_s=2\times 10^{19}\text{m}^{-3}$ and $P_{\text{rad}}=3\text{ MW}$. We note that the ratio of peak

heat loads between the horizontal and vertical targets is worse than that expected from the consideration of the change in wetted target surface alone.

CONCLUSIONS

For given n_s and P_{rad} , the presence or the shape of the septum does not influence appreciably most hydrogenic plasma parameters. For a recycling impurity introduced to increase radiation, the septum details likewise have little effect on impurity content. The shape of the septum does affect, however, the content of an intrinsic impurity such as carbon, affecting the approach to detachment and core contamination. Little difference is found between carbon and nitrogen for fixed P_{rad} , except for the fact that more C than N is required to radiate the same amount. There is not enough D flow, resulting from pumping and leakage, for impurity entrainment in the divertor, the low level of C retention, in particular, being mainly due to transport and not to the sputtering from the vessel wall outside the divertor. These conclusions hold for both vertical and horizontal targets, but in addition the horizontal targets have to sustain a much higher peak heat load. In any case, no solutions have been found with simultaneous detachment, high radiated power fraction and retention of impurities for Mark II GB in JET.

REFERENCES

- [1] R Simonini, G Corrigan, G Radford, J Spence, A Taroni, *Contrib. Plasma Phys.* 34(1994)368
- [2] E Deksnis, private communication
- [3] A Pospieszczyk, et al., *Proc. 22nd EPS Conf.* 19-II(1995)309

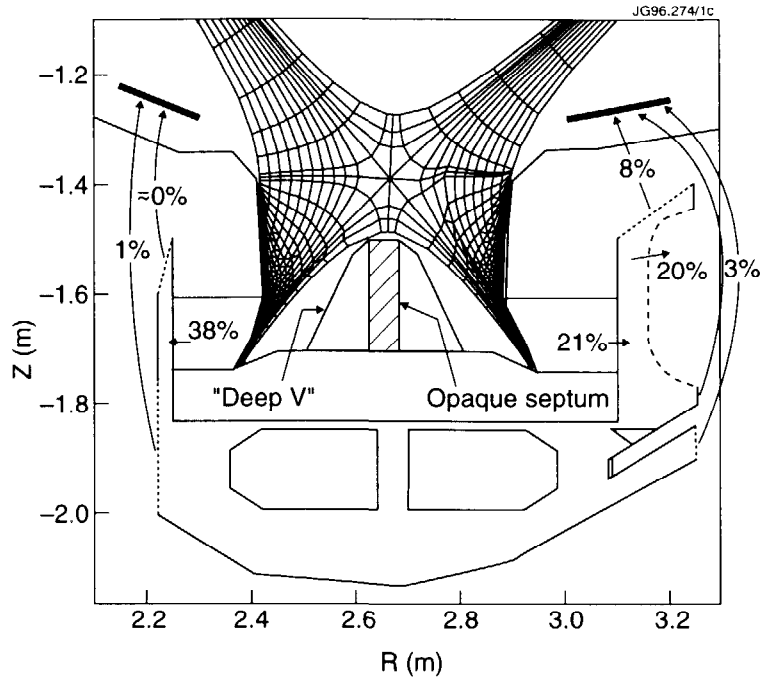


Fig.1. Vertical GB geometry, showing the three septum configurations, pumping and leakages

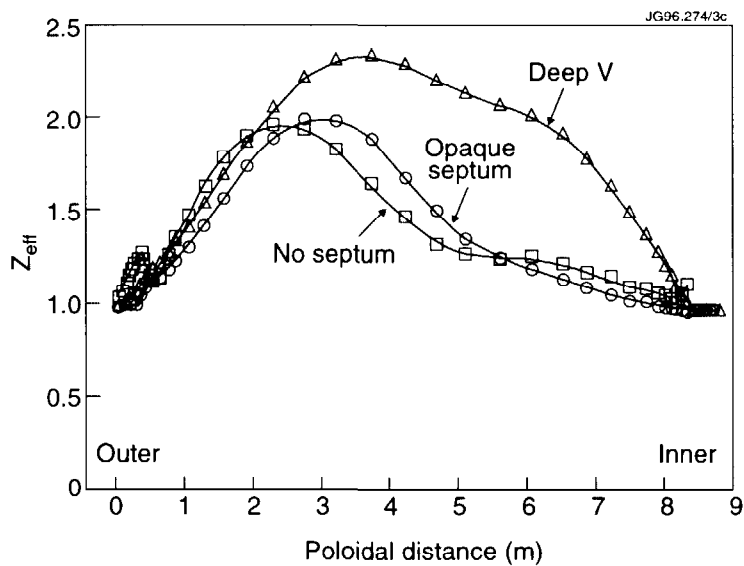


Fig.2. Poloidal profiles of Z_{eff} at separatrix with carbon as the radiating impurity for the three septum configurations. $n_s = 2 \times 10^{19} m^{-3}$, $P_i = P_e = 5 MW$

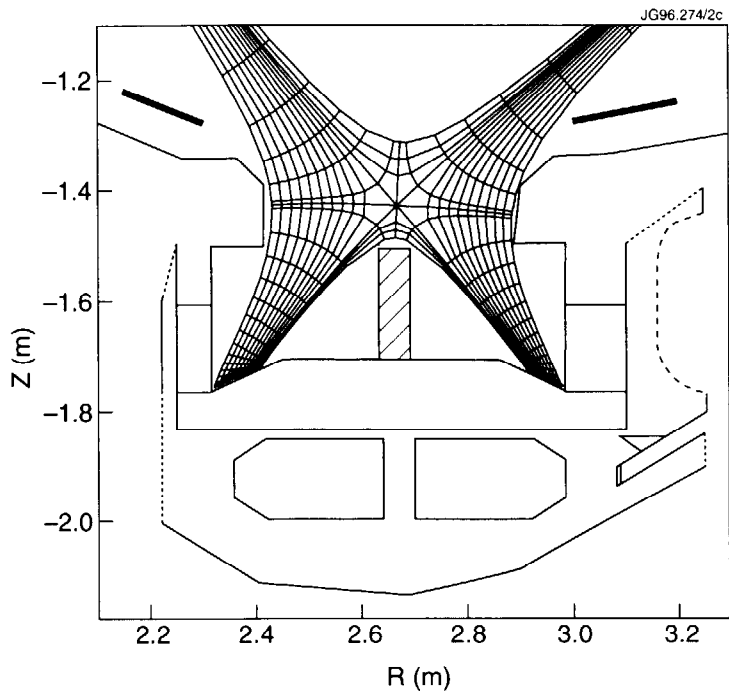


Fig.3. Horizontal GB divertor configuration

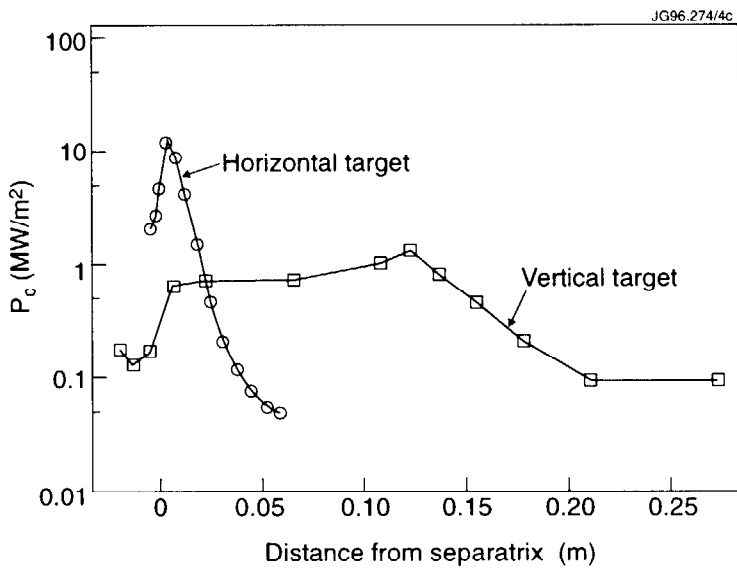


Fig.4. Heat loading on the outer divertor plate for the vertical and horizontal configurations, with nitrogen, $n_s=2 \times 10^{19} \text{ m}^{-3}$, $P_i=P_e=5 \text{ MW}$, $P_{rad}=3 \text{ MW}$